Sigma J Eng Nat Sci, Vol. 43, No. 4, pp. 1204−1210, August, 2025

Sigma Journal of Engineering and Natural Sciences
Web page info: https://sigma.yildiz.edu.tr
DOI: 10.14744/sigma.2025.00114

Research Article

A wideband bandstop filter design utilizing rounded interdigital meander lines and impedance stubs for S and C bands

Abdullah Selim KÖKSAL[1], Kamil KARAÇUHA[2,*], Şehabeddin Taha İMECİ[3]

[1]*Department of Electrical and Electronics Engineering, Fatih Sultan Mehmet Vakıf University, Istanbul, 34015, Türkiye*
[2]*Department of Electrical Engineering, Istanbul Technical University, Istanbul, 34467, Türkiye*
[3]*College of Engineering and Technology, American University of the Middle East, 15453, Kuwait*

ARTICLE INFO

Article history
Received: 02 July 2024
Revised: 14 August 2024
Accepted: 27 October 2024

Keywords:
Bandstop Filter; Filter Design; Interdigital Coupler; Meander Line; Rounded Interdigital

ABSTRACT

This paper introduces a novel wideband bandstop filter designed for S and C band applications, utilizing rounded interdigital meander lines and impedance stubs to achieve significant bandwidth and performance improvements. The proposed filter, with compact dimensions of 25 mm x 30 mm, exhibits a wide stopband spanning 4.58 GHz, covering critical frequencies for modern communication systems. The design leverages simple yet effective structural elements, including meandering lines and impedance stubs, to modify the impedance at the excitation ports, ensuring efficient band rejection. The filter's performance was thoroughly validated through parametric simulations, followed by the fabrication of a prototype on an FR4 substrate. Measurement results show excellent agreement with simulations, achieving $|S_{11}|$ of -0.56 dB and $|S_{21}|$ of -73 dB at 4 GHz, demonstrating the filter's ability to deliver high rejection with minimal insertion loss. This BSF not only offers a robust solution for interference mitigation in S and C bands but also stands out for its ease of fabrication and stability, making it a viable option for integration into compact and high-performance communication systems.

Cite this article as: Köksal AS, Karaçuha K, İmeci ŞT. A wideband bandstop filter design utilizing rounded interdigital meander lines and impedance stubs for S and C bands. Sigma J Eng Nat Sci 2025;43(4):1204−1210.

INTRODUCTION

Microwave filters are essential components in modern communication systems, enabling the selective transmission or blocking of signals within specific frequency ranges. This study focuses on the development of a wideband microstrip bandstop filter, utilizing stubs and meander lines to enhance performance. To further expand the bandwidth, a rounded interdigital meander line is incorporated into the design.

The literature contains extensive research on filter structures [1–4]. Recent studies provide an in-depth examination of advances in microwave filter design, showcasing a variety of techniques and methodologies. Dual-band filters have emerged as important solutions for addressing the needs of multi-frequency communication systems. For example, [5] introduces a dual-band bandstop filter that uses a circular, folded, meandered-line stepped-impedance resonator, which allows for precise control over

***Corresponding author.**
*E-mail address: karacuha17@itu.edu.tr

This paper was recommended for publication in revised form by Editor-in-Chief Ahmet Selim Dalkilic two resonant frequencies to achieve targeted signal rejection. Similarly, Compact dual-band bandstop filters using [6] presents compact dual-band bandstop filters with stepped-impedance resonators, offering multiple stopbands in a reduced-size design. A comparison of these approaches demonstrates their effectiveness in achieving dual-band functionality while minimizing physical size.

Bandstop filters are particularly useful for reducing interference from specific frequency bands. Studies such as [7] and [8] explore reconfigurable and compact bandstop filters using defected microstrip structures and interdigital resonators. These designs provide tunable central frequencies and excellent band rejection capabilities, catering to a wide range of communication needs. Comparative analysis reveals the trade-offs between reconfigurability and compactness, providing insights into choosing filters for specific applications.

Bandpass filters also play a crucial role in allowing signal transmission within desired frequency bands. References [9–11] introduce innovative bandpass filter designs, employing novel resonator structures and coupling techniques to achieve compactness, selectivity, and improved stopband performance. Through comparative analysis, the trade-offs between filter size, selectivity, and insertion loss are highlighted, aiding in the selection of suitable designs for specific applications.

Wideband filters are particularly important for systems requiring transmission across broad frequency ranges. Works such as [12] and [13] examine the design of compact ultrawideband filters with high selectivity and wide stopbands, addressing the demands of emerging communication technologies like 5G NR. A comparative evaluation of these designs highlights the balance between bandwidth, selectivity, and stopband suppression, guiding the selection of wideband filters.

Hybrid components, like the 90° hybrid branch-line coupler discussed in [14], offer high-performance characteristics in compact designs, making them ideal for integration into modern communication systems. Comparative analysis highlights the advantages of hybrid components over traditional designs, particularly for applications with size constraints. Finally, advancements in compact filter designs are evident in studies such as [15] and [16], which propose novel microstrip structures for bandstop and bandpass filters. These designs maintain small footprints while meeting critical performance metrics for reliable communication. Comparative assessments provide insights into the balance between filter size, complexity, and performance, supporting the selection of optimal designs for specific applications.

Recent developments in filter design have focused on compactness, performance, and enhanced selectivity for modern wireless communication systems. In [6], a dual-band bandstop filter with stepped-impedance resonators achieves a 12.6% size reduction while maintaining controllable stopbands. In contrast, [8] presents an ultra-wideband bandpass filter using half-mode substrate integrated waveguide (HMSIW) structures, which offers a broad passband and wide stopband. Similarly, [11] introduces a wideband bandpass filter for 5G bands with tunable bandwidth via varactor diodes. While [12] explores a microstrip λ/4 interdigital structure for a wide passband and suppression of spurious frequencies, [16] uses a hybrid multilayer HMSIW filter for high selectivity, introducing transmission zeros for sharper filtering.

Despite different approaches, these designs all aim to improve size, selectivity, and suppression of unwanted frequencies, addressing key challenges in modern communication systems. This study offers a simple, compact, and stable solution for wideband stopband filtering by combining rounded meander lines with impedance stubs. The novelty of this design lies in merging these two classical methods to create a highly efficient bandstop structure. The proposed filter meets several important performance criteria, as described in the following sections. This wideband bandstop filter is especially well-suited for applications in modern communication systems, such as mitigating interference in 5G networks and satellite communication systems operating within the S and C bands. Additionally, the filter can improve signal quality in wireless communication infrastructure by rejecting unwanted frequencies, thereby enhancing overall system performance in both commercial and defense applications.

This paper is structured as follows: the next sections discuss the design process of the proposed filter, followed by simulation results optimized for various parameters. Measurement results are then presented, and comparisons with existing literature are provided. The paper concludes with a summary of the findings.

DESIGN OF THE FILTER

We utilized the Sonnet program to both design and simulate our filter. Although sharing core similarities with existing filters, our goal was to bolster its ability to reject a wide range of signals. However, adapting the filter to suit the 1mm thick FR4 substrate (the only available substrate for manufacturing in the research laboratory) required specific adjustments, adding complexity to the design process. The design process began with the matching of 50-ohm transmission line widths to the input and output ports, ensuring optimal impedance matching. Subsequently, two symmetric vertical stubs were incorporated to further enhance impedance matching. Finally, the S-shaped center separations were carefully adjusted, as these are known to play a critical role in the current distribution of bandstop filters, significantly influencing the filter's overall performance.

In our pursuit of optimizing the performance of the proposed bandstop filter, employing a rounded interdigital gap on the FR4 with a 4 GHz bandwidth, we meticulously analyzed and modified various design parameters [17,18]. These parameters encompassed the interdigital gap's dimensions, transmission line width, and the overall structural geometry of the filter. Through iterative adjustments guided by simulation tools, we aimed to achieve the desired bandstop characteristics within the 4 GHz bandwidth [19–21].

The design of the microstrip filter relies significantly on several critical formulas pivotal to this process provided as (1) and (2) below. Accurate application of these foundational equations is paramount for obtaining the desired filter properties. Our design strategy revolves around the following formulas [1,18]:

$$Z_0 = 1 + \frac{87}{\sqrt{(\varepsilon_r + 1.41)}} \ln \frac{5.98 \times h}{0.8 \times w + t} \tag{1}$$

Here, Z_0 is the characteristic impedance of the transmission line. Besides, h, w and t stand for the thickness of the dielectric substrate, the width of the transmission line, and, the thickness of the cladding of the metallic surface, respectively. Furthermore, effective epsilon value can be obtained as:

$$\varepsilon_{eff} = \frac{\varepsilon_r + 1}{2} + \frac{\varepsilon_r - 1}{2}\left(1 + 12\left(\frac{h}{w}\right)\right)^{-\frac{1}{2}}. \tag{2}$$

Besides, we extensively assessed the influence of the FR4 substrate on the filter's performance [12]. We meticulously considered the dielectric properties of FR4, including its relative permittivity and loss tangent, to ensure precise modeling and simulation outcomes. This analysis allowed us to fine-tune the filter's design and optimize its performance tailored to the characteristics of the specific substrate material [20]. For a visual representation, refer to Figure 1 depicting the filter's three-dimensional view. The dimensions of the rectangle in the center of the filter are 10.6x10.1 mm, and the meander gap separation is 0.25 mm. The bottom layer is copper cladding and is employed as a ground plate.

The design process followed a systematic approach, involving iterative refinements of the filter's geometry while taking into account the distinct attributes of the FR4 substrate. We relied on simulation tools extensively to validate the filter's performance. This design methodology aimed to craft an effective bandstop filter with rounded interdigital gaps, specifically engineered to function within the targeted 4 GHz bandwidth.

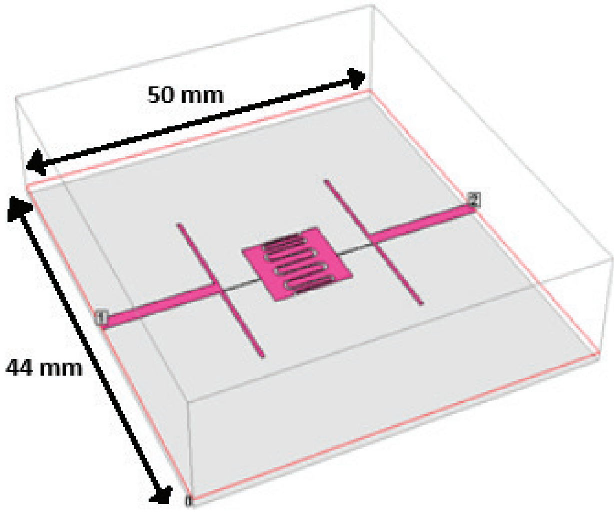

Figure 1. The 3D view of the filter.

SIMULATION RESULTS

The S-parameters graph of the final design has a 4.24 GHz bandwidth between 2.75 and 6.99 GHz. The minimum input match that the bandwidth reaches is -60 dB. The graph in Figure 2 shows the graphical results of the filter. Figure 2 The simulated S-parameters (in dB) versus the frequency graph of the bandstop filter (the red curve is $|S_{11}|$ and the blue curve is $|S_{21}|$). We utilized Sonnet software for the complete design, development, and simulation of our filter. The simulation settings involved conducting a frequency sweep and a parametric study on the filter design.

Figure 3 presents the current distribution across the filter, offering insights into its behavior. On the other hand, Figure 4 provides a top view of the filter, showcasing the details of the parametric study conducted during our simulation.

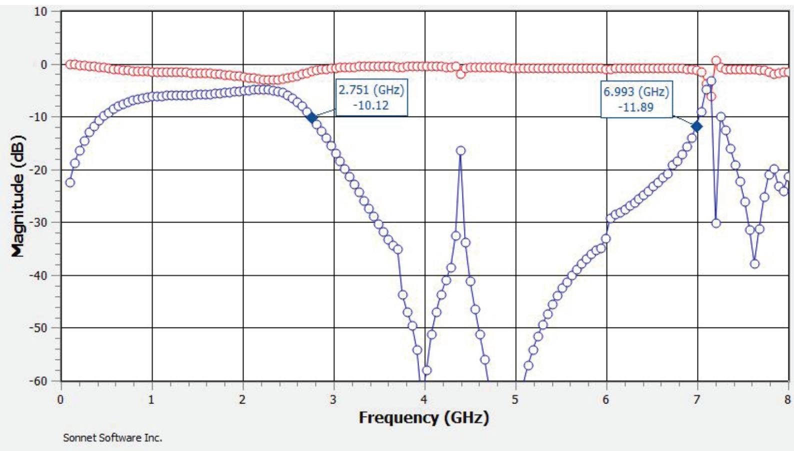

Figure 2. Simulated $|S_{11}|$ and $|S_{21}|$ parameters of the structure.

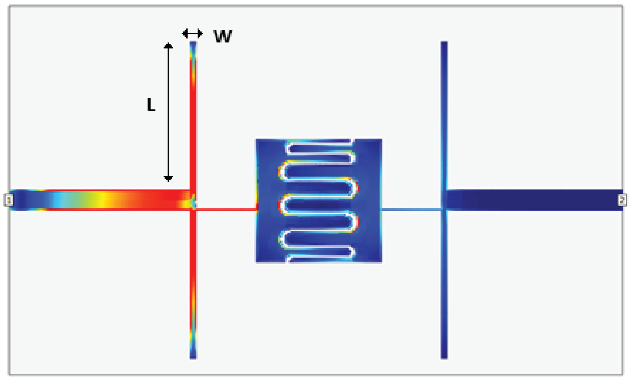

Figure 3. Current distribution of the filter at 4 GHz (port at left is excited only).

PARAMETRIC STUDY

In Figure 3, the top view of the filter is depicted. To initiate the parametric design, we configured the variables W and L within the simulation software to span across various values. The tables below showcase the outcomes resulting from the diverse values explored during the parametric study. In Tables 1 and 2, parametric studies about *W* and *L* are provided, respectively. As can be seen from the tables, parameters *W* and *L* have a crucial impact on the design. Two of the main design parameters are *W* and *L* due to their profound effect on the bandwidth and scattering parameters. The parameter *W* determines the bandwidth whereas *LL* optimizes the scattering parameters.

Table 1. Parametric study on the width (*W*)

W (mm)	Relative dielectric constant (ε_r)	$\lvert S_{11}\rvert$ (dB)	$\lvert S_{21}\rvert$ (dB)	BW (GHz)
0.2	4.4	-1.2dB	-23dB	4.12
0.4	4.4	-1.1dB	-24dB	4.24
0.6	4.4	-1.3dB	-23dB	4.17
0.8	4.4	-1.4dB	-22dB	4.08
1	4.4	-1.5dB	-21dB	3.98

Table 2. Changes made to the length (*L*)

L (mm)	Relative dielectric constant (ε_r)	$\lvert S_{11}\rvert$ (dB)	$\lvert S_{21}\rvert$ (dB)	BW (GHz)
8	4.4	-7dB	-6dB	4.1
9	4.4	-2.6dB	-13dB	4.24
10	4.4	-1.1dB	-24dB	4.16
11	4.4	-1.1dB	-27dB	4.1
12	4.4	-1.1dB	-28dB	4.24

Parametric Results

The fabrication process involved constructing the bandstop filter on a standard FR4 dielectric substrate using the milling machine, showcasing the practical feasibility of our proposed concept. The chosen FR4 substrate had specific characteristics: a dielectric constant (ε_r) of 4.4, a thickness (h) of 1 mm, and a loss tangent (tan) of 0.02. These specifications were deliberately selected to ensure compatibility with common manufacturing practices, streamlining the production process.

Employing the milling machine for fabrication allowed us to create the filter structure on a 1mm-thick FR4 substrate. This fabrication approach was aimed at offering a practical solution for manufacturing the bandstop filter. The simplicity and ease provided by both the chosen substrate and the milling machine pave the way for scalability and reproducibility in future production processes. Figure 4 has the fabricated picture of the filter.

After fabricating the filter with the milling machine, we undertook an additional fabrication using the toner transfer method, involving a laserjet printer, a laminating machine, and label paper. This method comprises printing our design onto label paper using the printer. Subsequently, we laminate the printed label paper onto the FR4 substrate to transfer the ink from the paper to the substrate. Following this, the FR4 substrate carrying our design negative is placed into an etchant solution, which comprises a mixture of hydrochloric acid and hydrogen peroxide. For the solution, we combine 120 grams of hydrochloric acid with 70 grams of hydrogen peroxide within a container holding the substrate. After an elapsed time of approximately 2-4 minutes, our filter is successfully imprinted on the substrate.

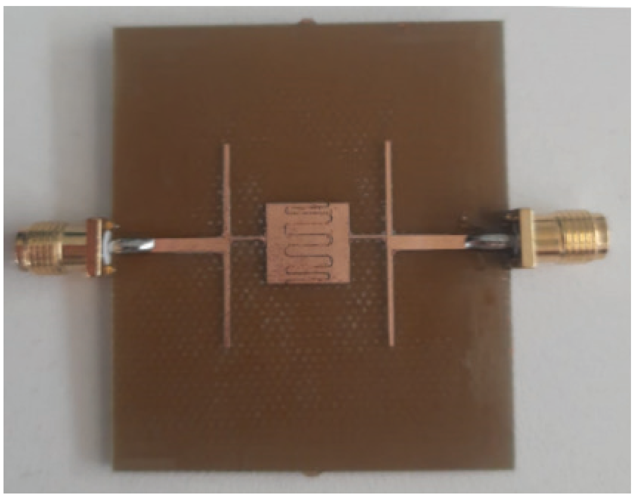

Figure 4. The fabricated design of the proposed filter with the milling machine.

Overall, both the milling machine and the toner transfer method were utilized to successfully fabricate the bandstop filter, providing different manufacturing options based on specific requirements and available resources.

Measurements Results

The image presented in Figure 5 shows a visual of our measurement of the filter that was fabricated with the milling machine. The fabricated bandstop filter, presented in Figures 5 and 6, revealed that our filter's $|S_{21}|$ values closely matched those observed in the simulation software, as depicted in Figure 2. However, our $|S_{11}|$ values did not align with our initial expectations. Subsequently, we proceeded to fabricate and measure another filter using the toner transfer method.

Addressing the performance of the previous filter, we conducted measurements using the newly fabricated filter, yielding exceptional outcomes for an FR4 substrate-based filter. Notably, we achieved a superior bandwidth compared to the simulation results. Additionally, the absence of a second notch in the middle of the $|S_{21}|$ indicated a marked improvement in the filter's performance. In our research's measurement phase, we conducted a comparison between the simulated and measured values of the $|S_{21}|$ and $|S_{11}|$ parameters for our filter. Remarkably, the simulation results closely aligned with the actual measured values, signifying a high level of precision in our design. Figure 6 distinctly portrays the remarkable concurrence between the simulated and measured $|S_{21}|$ and $|S_{11}|$ values. This near-match between the simulated and measured data affirms the dependability and efficiency of our filter design. The simulation and the measurement results coincide. As expected, the produced prototype under test is operating properly in-band as designed. The deviations in the operating band are generally at a higher frequency regime since FR4 is a lossy material and the production errors may affect more at a higher frequency regime.

The consistency observed in the performance between the simulated and measured results validates the accuracy of our simulation model. It underscores the successful realization of our proposed filter. The slight decline in high frequencies of the $|S_{11}|$ parameter is likely attributed to the inherent lossy characteristic of the FR4 substrate.

In summary, our research yielded two sets of measured filter data due to unexpected values obtained from our initial filter. Consequently, we proceeded to fabricate and measure the filter using an alternative FR4 substrate available to us. Post-measurement analysis revealed that our latest filter outperformed the previous one and was notably easier to fabricate, primarily owing to the rounded corners of the interdigital coupler. This design detail took longer to fabricate using the milling machine. Our measurements were conducted utilizing a Rohde & Schwarz ZVL network analyzer.

Several recent studies have contributed significantly to the development of wideband filter technology for diverse frequency band applications (see Table 3). Zhou et al. [8] and Golestanifar et al. [11] showcased similar wide-band band-pass filter (BPF) designs spanning 3.15 to 6.05 GHz, catering to 5G NR frequency bands n77, n79, and 5G Wi-Fi, achieving low insertion loss (IL), good and stable return loss (RL), sharp roll-off rates, and suppression of unwanted harmonics up to 12 GHz. In contrast, Lin & Dong [16]

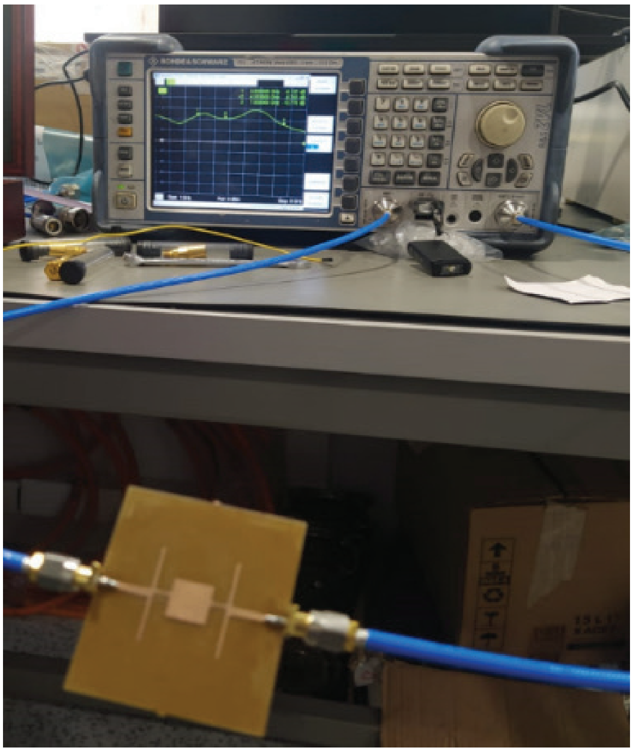

Figure 5. Measurement of the filter fabricated with the milling machine.

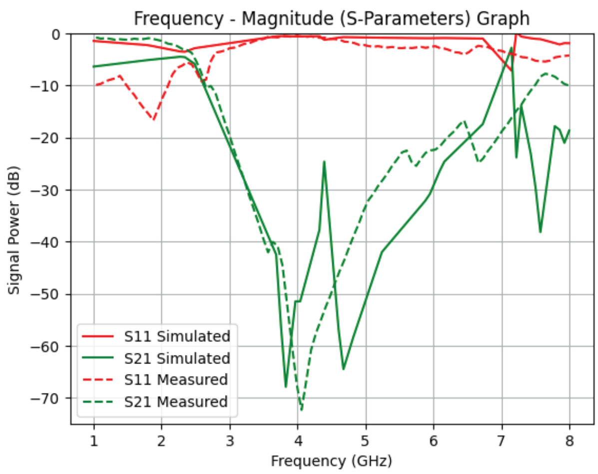

Figure 6. Comparison of S-parameters (in dB) versus frequency between measured and simulated results of the filter.

Table 3. Comparisons with other studies

Ref.	3 dB FBW (%)	f_0 (GHz)	ε_r	IL (dB)	RL (dB)	Size (mm^3)	Size (λ^3_d)
Zhou C-X et al. [8]	110.1	6.85	3.55	< 1.6	>12	16 × 14.5 × 0.51	$0.688\lambda_d \times 0.624\lambda_d \times 0.022\lambda_d$
Golestanifar A et al. [11]	62.6	4.585	3.55	< 2	>15	16.9 × 16.7 × 0.8	$0.487\lambda_d \times 0.481\ \lambda_d \times 0.023\ \lambda_d$
Gu L et al. [16]	10	10.71	2.2	1.57	>15	23.5 × 12.6 × 1.1	$1.244\lambda_d \times 0.667\lambda_d \times 0.058\lambda_d$
Li C et al. [21]	40.33	12.795	3.66	0.58	>18	20.8 × 20 × 1.3	$1.697\ \lambda_d \times 1.631\lambda_d \times 0.106\lambda_d$
Our work	45.8	4	4.4	0.56	>70	25 × 30 × 1	$0.699\lambda_d \times 0.839\lambda_d \times 0.027\ \lambda_d$

innovatively employed a hybrid multilayer half-mode substrate-integrated waveguide (HMSIW) for enhanced selectivity, achieving a fourth-order response and improved stopband performance. Li et al.'s [21] work introduced a compact ultra-wideband bandpass filter using a multilayer printed circuit board (MPCB) structure, demonstrating low insertion loss and a wide fractional bandwidth from 10.215 GHz to 15.375 GHz. These studies reflect diverse methodologies and advancements, emphasizing bandwidth control, improved selectivity, and performance enhancements for various wireless communication applications. The comparison of these studies with the proposed study is provided in Table 3 (dimensions are provided in terms of both millimeters and guided wavelength).

CONCLUSION

This research successfully introduced a novel wideband bandstop filter with rounded interdigital gaps, specifically designed for S and C band applications on an FR4 substrate. Through meticulous design and simulation using Sonnet electromagnetic simulation software, the proposed filter achieved a 4.58 GHz stopband with excellent rejection capabilities, evidenced by an |S11| of -0.56 dB and S21 of -73 dB at 4 GHz. The fabrication process, which involved both the milling machine and toner transfer methods, played a crucial role in validating the design. The filter produced via the milling machine closely matched the simulated results, but further refinement using the toner transfer method yielded even better performance, demonstrating a wider bandwidth and more efficient fabrication due to the smoother, rounded interdigital gaps. This refined process ensured scalability and repeatability, highlighting the filter's potential for practical applications in modern communication systems, such as interference mitigation in 5G networks, satellite communication systems, and radar applications operating within the S and C bands. The wideband nature of the filter makes it particularly suited for communication systems requiring interference suppression across multiple bands, improving signal quality by rejecting unwanted frequencies. It can be integrated into modern wireless communication infrastructure, including base stations, satellite receivers, and other RF systems that operate in congested frequency environments, ensuring stable and reliable signal transmission. The consistency between the simulated and measured results underscores the accuracy of the design and fabrication process, making this bandstop filter a reliable and high-performance solution for S and C band applications. This research not only advances wideband filter technology but also offers a scalable approach to RF filtering, providing a strong foundation for future developments in communication system filters.

ACKNOWLEDGEMENTS

We would like to thank SONNET Software for licensing the electromagnetic simulation tool for Fatih Sultan Mehmet Vakıf University, our university research center BETAM for the fabrication, and PROFEN A.Ş. for the measurements.

AUTHORSHIP CONTRIBUTIONS

Authors equally contributed to this work.

DATA AVAILABILITY STATEMENT

The authors confirm that the data that supports the findings of this study are available within the article. Raw data that support the finding of this study are available from the corresponding author, upon reasonable request.

CONFLICT OF INTEREST

The author declared no potential conflicts of interest with respect to the research, authorship, and/or publication of this article.

ETHICS

There are no ethical issues with the publication of this manuscript.

STATEMENT ON THE USE OF ARTIFICIAL INTELLIGENCE

Artificial intelligence was not used in the preparation of the article.

REFERENCES

[1] Pozar DM. Microwave engineering: theory and techniques. New York: John Wiley & Sons; 2021.

[2] Çelik FT, Karaçuha K. Broadband RF communication system design for smart houses including Wi-Fi and 5G. In: 2019 Photonics & Electromagnetics Research Symposium-Fall (PIERS-Fall); 2019. p. 1558–1562. IEEE. [CrossRef]

[3] Bandar H, Tokan NT. Comparison of post and iris substrate integrated waveguide band-pass filters for X-Band applications. Sigma J Eng Nat Sci 2022;40:45–56.

[4] Belen MA, Mahoutı P, Partal HP, Demirel S, Güneş F. Design and simulation of a tunable bandpass filter using varactor diodes for wireless and radar applications. Sigma J Eng Nat Sci 2015;33:86–93.

[5] Dhakal R, Kim N. A compact dual-band bandstop filter using a circular, folded, symmetric, meandered-line, stepped-impedance resonator. Microw Opt Technol Lett 2014;56:2298–301. [CrossRef]

[6] Chin K-S, Yeh J-H, Chao S-H. Compact dual-band bandstop filters using stepped-impedance resonators. IEEE Microw Wirel Compon Lett 2007;17:849–851. [CrossRef]

[7] Elashry GM, Abd-El-Hadi AA, Abdallah EA. Compact reconfigurable triple bandstop filter using defected microstrip structure (DMS). Prog Electromagn Res C 2023;136. [CrossRef]

[8] Zhou C-X, Guo P-P, Zhou K, Wu W. Design of a compact UWB filter with high selectivity and superwide stopband. IEEE Microw Wirel Compon Lett 2017;27:636–638. [CrossRef]

[9] Yan J-M, Kang B-J, Yang Y, Cao L. Single- and dual-band bandpass filters based on a novel microstrip loop-type resonators loaded with shorted stubs. Prog Electromagn Res Lett 2023;113. [CrossRef]

[10] Velazquez-Ahumada M, Martel-Villagran J, Medina F, Mesa F. Application of stub loaded folded stepped impedance resonators to dual band filters. Prog Electromagn Res 2010;102:107–124. [CrossRef]

[11] Golestanifar A, Karimi G, Lalbakhsh A. Varactor-tuned wideband band-pass filter for 5G NR frequency bands n77, n79 and 5G Wi-Fi. Sci Rep 2022;12:16330. [CrossRef]

[12] Liang C-H, Chang C-Y. Compact wideband bandpass filters using stepped-impedance resonators and interdigital coupling structures. IEEE Microw Wirel Compon Lett 2009;19:551–553. [CrossRef]

[13] Yoon K, Kim K. Compact size of an interdigital band-pass filter with flexible bandwidth and low insertion-loss using a folded spiral and stepped impedance resonant structure. Electronics (Basel) 2021;10:2003. [CrossRef]

[14] Farhat M, Virdee BS, Ghareeb NH. Microstrip bandpass filter with wide stopband and high out-of-band rejection. Am J Eng Appl Sci 2019;12:543–548. [CrossRef]

[15] Ünal ÜC, Karaçuha K, İmeci ST. A simple 90° hybrid branchline coupler with wideband phase balance for 5G applications. J Electr Eng 2024;75:86–93. [CrossRef]

[16] Gu L, Dong Y. Compact half-mode SIW filter with high selectivity and improved stopband performance. IEEE Microw Wirel Compon Lett 2022;32:1039–1042. [CrossRef]

[17] Çelik FT, Joof S, Karaçuha K. A dual-polarized bandwidth enhanced filtering dipole antenna design for 5G. IEEE Access 2023;11:78754–78767. [CrossRef]

[18] Collin RE. Foundations for Microwave Engineering. New York: John Wiley & Sons; 2007.

[19] Yang R-Y, Weng M-H, Hung C-Y, Chen H-J, Houng M-P. Novel compact microstrip interdigital bandstop filters. IEEE Trans Ultrason Ferroelectr Freq Control 2004;51:1022–1025. [CrossRef]

[20] Matthaei GL, Young L, Jones EMT. Impedance-matching networks, and coupling structures. Norwood, Massachusetts, United States: Artech House Books; 1964. p. 497–506. [CrossRef]

[21] Li C, Ma Z-H, Chen J-X, Wang M-N, Huang J-M. Design of a compact ultra-wideband microstrip bandpass filter. Electronics (Basel) 2023;12:1728. [CrossRef]